THE JOURNAL OF PHYSICAL CHEMISTRY A
A JOURNAL OF THE AMERICAN CHEMICAL SOCIETY

pubs.acs.org/JPCA Article

$^{1}H/^{17}O$ Chemical Shift Waves in Carboxyl-Bridged Hydrogen Bond Networks in Organic Solids

Gang Wu,* Yizhe Dai, Ivan Hung, Zhehong Gan, and Victor Terskikh

Cite This: *J. Phys. Chem. A* 2024, 128, 4288−4296 Read Online

ACCESS | Metrics & More | Article Recommendations | Supporting Information

ABSTRACT: We report solid-state ^{1}H and ^{17}O NMR results for four ^{17}O-labeled organic compounds each containing an extensive carboxyl-bridged hydrogen bond (CBHB) network in the crystal lattice: tetrabutylammonium hydrogen di-[$^{17}O_2$]-salicylate (**1**), [$^{17}O_4$]quinolinic acid (**2**), [$^{17}O_4$]dinicotinic acid (**3**), and [$^{17}O_2$]Gly/[$^{17}O_2$]Gly·HCl cocrystal (**4**). The ^{1}H isotropic chemical shifts found for protons involved in different CBHB networks are between 8.2 and 20.5 ppm, which reflect very different hydrogen-bonding environments. Similarly, the ^{17}O isotropic chemical shifts found for the carboxylate oxygen atoms in CBHB networks, spanning a large range between 166 and 341 ppm, are also remarkably sensitive to the hydrogen-bonding environments. We introduced a simple graphical representation in which ^{1}H and ^{17}O chemical shifts are displayed along the H and O atomic chains that form the CBHB network. In such a depiction, because wavy patterns are often observed, we refer to these wavy patterns as $^{1}H/^{17}O$ chemical shift waves. Typical patterns of $^{1}H/^{17}O$ chemical shift waves in CBHB networks are discussed. The reported ^{1}H and ^{17}O NMR parameters for the CBHB network models examined in this study can serve as benchmarks to aid in spectral interpretation for CBHB networks in proteins.

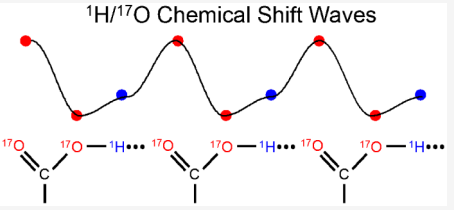

1. INTRODUCTION

In 1936, Huggins[1] postulated the existence of carboxyl-bridged hydrogen bond (CBHB) networks as possible alternative structures to the more commonly found carboxylic acid head-to-head (or cyclic) dimer formation. The crystal structures of anhydrous α- and β-oxalic acids were early examples, illustrating the difference between the two hydrogen-bonding motifs (i.e., CBHB network versus dimer formation).[2,3] In the crystal lattice of anhydrous α-oxalic acid, oxalic acid molecules form hydrogen-bonded dimers in a head-to-head fashion. Because of the bifunctionality of the oxalic acid molecule, hydrogen-bonded dimers are further connected by tail-to-tail hydrogen bonding to the adjacent dimers so that the oxalic acid dimers form a continuous ribbon along the crystallographic b-axis. Thus, the basic hydrogen-bonding motif in anhydrous α-oxalic acid is dimer formation. For anhydrous β-oxalic acid, on the other hand, each end of the oxalic acid molecule serves as a HB donor in the sideways, forming a one-dimensional CBHB chain, as illustrated in Scheme 1a. Huggins[1] further mentioned the two possible CBHB networks based on the symmetry in the O−H···O HB (i.e., O−H···O vs O^{-}···H^{+}···O^{-}). For amino acids where both carboxyl and amino functional groups are present, the CBHB network can also include the amino groups, as depicted in Scheme 1c. Such CBHB networks are sometimes referred to as catemers.[4]

In fact, CBHB networks are quite commonly found not only in organic solids[5] but also in proteins.[6,7] In recent years, an increasing number of ultrahigh resolution X-ray crystal structures and neutron crystal structures of proteins have been reported in the literature. As a result, it has become clear that the

Scheme 1. Several CBHB Networks Postulated by Huggins[1] for Carboxylic Acids in the Solid State

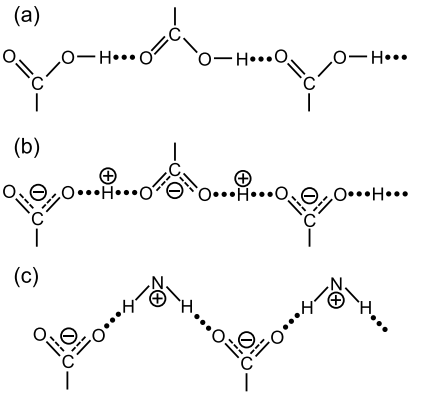

CBHB motifs in proteins may play important roles in biological functions. Here, we briefly show three examples to illustrate the characteristic CBHB networks observed in proteins. First, in the 1.12 Å resolution X-ray structure of rhamnogalacturonan acetylesterase (PDB entry 1k7c), Langkilde et al.[6] observed a

Received: March 21, 2024
Revised: April 25, 2024
Accepted: May 3, 2024
Published: May 15, 2024

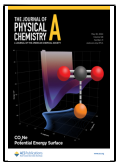

https://doi.org/10.1021/acs.jpca.4c01866
J. Phys. Chem. A 2024, 128, 4288−4296

CBHB network between the Gly72 backbone NH and the carboxyl groups of Asp75 and Asp87; see Scheme 2a. The Gly72

Scheme 2. Three Examples of CBHB Networks Found in Proteins: (a) 1k7c, (b) 4kxw, (c) 5mop

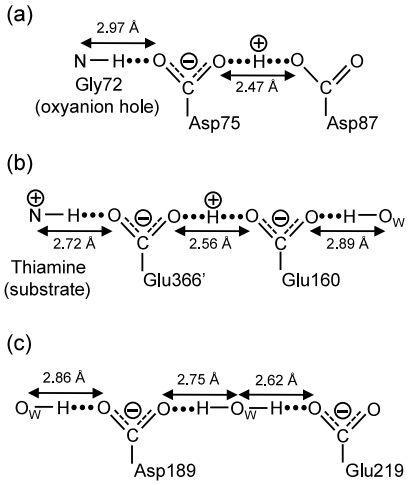

is a key residue forming the oxyanion hole. The authors further identified the ^{1}H NMR signal at 18 ppm to be due to the proton in the short O−H···O HB between Asp75 and Asp87. Second, in the ultrahigh resolution X-ray structure of human transketolase (PDB entry 4kxw), Dai et al.[8] observed a putative hydrogen-bonded proton wire linking the two active sites of the protein dimer over a distance of about 25 Å. The entire HB network of this proton wire consists of six glutamate groups and several water molecules. Scheme 2b shows a portion of the CBHB network. The thiamine cofactor is protonated by the canonical catalytic residue, Glu366′, which is then hydrogen bonded to Glu160 with a very short O···O distance of 2.56 Å. More importantly, the ultrahigh resolution structure allowed the authors to detect the key proton, which appears to be at the midpoint between the two oxygen atoms. Glu160 is further hydrogen bonded to a water molecule. The third example is the combined X-ray/neutron structure of apo-trypsin (PDB entry 5mop).[9] As seen in Scheme 2c, Schiebel et al.[9] observed that in the empty S_1 pocket of trypsin, Asp189, Glu219, and two water molecules form a CBHB network. In this work, the neutron diffraction data allowed the authors to determine the proton positions in the key water molecules. Another related example is the debate about the detailed HB network around the catalytic Asp 25-Asp 25′ dyad in pepstatin A/HIV-1 protease complex.[10−12]

Carboxylic acid dimers have been extensively studied by many researchers with different spectroscopic techniques for several decades.[13−39] The main focus in the majority of these studies was the double proton tunneling phenomenon within each hydrogen-bonded carboxylic acid dimer. Among the various spectroscopic techniques used so far to study this phenomenon, solid-state NMR has been shown to be of particular importance.[40−43] While ^{1}H is the most common NMR probe in studies of carboxylic acid dimers, solid-state ^{17}O NMR has recently emerged as another powerful technique for probing hydrogen bonding interactions.[44−54] Indeed, several solid-state ^{17}O NMR investigations of carboxylic acids have been reported in the literature.[55−68] We should note that ^{17}O nuclear quadrupole resonance (NQR) spectroscopy has also been used to study carboxylic acid dimers.[69−71] It is generally appreciated that the cooperativity in an extended HB network (such as the extended HB network in ice or the "water wires" in proteins) may result in new spectral properties that are distinct from those exhibited by an isolated HB. Surprisingly, despite the fact that many of the CBHB networks are structurally characterized both in organic solids and in proteins as mentioned earlier, they have been rarely studied by spectroscopic methods. We should point out that there has been an intense interest in the symmetry of the HB formed in acid salts of carboxylic acids in the form of [O═C−O···H···O−C═O]$^{-}$.[72−78] Clearly, as seen in Scheme 2, this particular structural motif can be considered to be a major component of the CBHB network. In the present work, we use solid-state ^{1}H and ^{17}O NMR to study several typical CBHB networks found in organic solids. Because the hydrogen bonding in CBHB networks is most often of the O−H···O (or O^{-}···H^{+}···O^{-}) type, the combined use of solid-state ^{1}H and ^{17}O NMR should allow us to obtain the most complete information about the NMR spectral properties in CBHB networks. This general approach was recently demonstrated in studies of hydrogen bonding in 1,3-diketone compounds.[79,80] The CBHB networks chosen in this study also resemble those seen in proteins. The goal of this study is to collect fundamental ^{1}H and ^{17}O NMR parameters for CBHB networks and to investigate possible spectral patterns that can be linked to the characteristic structural features of CBHB networks. As ^{17}O NMR has become a direct tool for studying proteins and ligand−enzyme complexes,[81−87] information collected for a few carefully chosen CBHB models may be used as benchmarks for future ^{1}H and ^{17}O NMR studies of CBHB networks in proteins.

2. EXPERIMENTAL DETAILS

2.1. Synthesis. Tetrabutylammonium hydrogen di-[$^{17}O_2$]-salicylate (**1**) was prepared in the following fashion. [$^{17}O_2$]-Salicylic acid was prepared with a previously reported procedure.[62] To an acetone solution (4 mL) containing 507 mg of [$^{17}O_2$]salicylic acid was slowly added 4 mL of 0.4 M tetrabutylammonium hydroxide(aq) (prepared from solid tetrabutylammonium hydroxide·30 H_2O) while stirring. After the solution was evaporated to dryness, the solids were redissolved in 2 mL of water. After extraction with dichloromethane (3 × 2 mL), the organic portion was evaporated to produce white solids of **1**.

[$^{17}O_4$]Quinolinic acid ([$^{17}O_4$]pyridine-2,3-dicarboxylic acid) (**2**) was prepared by base-catalyzed hydrolysis of dimethyl 2,3-pyridinedicarboxylate. In particular, 200 mg of dimethyl 2,3-pyridinedicarboxylate was dissolved in 3 mL of MeOH in a pressure tube. To the solution were added 100 mg of NaOH(s) and 200 μL of ^{17}O-enriched H_2O (40% ^{17}O from CortecNet). The reaction solution appeared cloudy. The pressure tube was then left in an oil bath at 90 °C for 7 h. After the pressure tube cooled to room temperature, small aliquots of 1 M HCl(aq) were added gradually while stirring until the reaction solution reached pH ∼ 2. At this point, the solution was clear. The solution was dried with a gentle flow of the N_2 gas. The solids were briefly washed with 0.5 mL of cold H_2O and dried in a desiccator over P_2O_5 for 1 day (yield: 75%).

[$^{17}O_4$]Dinicotinic acid ([$^{17}O_4$]pyridine-3,5-dicarboxylic acid) (**3**) was prepared in a similar way as the ^{17}O-labeling of nicotinic acid reported previously.[65]

[$^{17}O_2$]Gly/[$^{17}O_2$]Gly·HCl cocrystal (**4**) was prepared in the following fashion. To a pressure tube were added 2 mL solution

https://doi.org/10.1021/acs.jpca.4c01866
J. Phys. Chem. A 2024, 128, 4288−4296

of 4 M HCl in dioxane, glycine (500 mg, 1 mmol), and $H_2{}^{17}O$ (1 g, 53 mmol, 40% ^{17}O atom). The tube was placed in an oil bath at 70 °C for 24 h with magnetic stirring. The reaction mixture was then evaporated to dryness, resulting in [$^{17}O_2$]Gly·HCl (510 mg, 95% yield). A portion of [$^{17}O_2$]Gly·HCl was then converted to [$^{17}O_2$]Gly by passing it through a column loaded with ion-exchange resin (poly-4-vinylpyridine). The final [$^{17}O_2$]Gly/[$^{17}O_2$]Gly·HCl cocrystal was obtained by mixing [$^{17}O_2$]Gly and [$^{17}O_2$]Gly·HCl in a 1:1 molar ratio and crystallized from water.

2.2. Solid-State NMR Measurement. All solid-state ^{1}H NMR spectra were obtained under magic-angle spinning (MAS) conditions on a Bruker NEO-700 spectrometer equipped with a Bruker 2.5 mm HX MAS probe (typical sample spinning frequency of 30 kHz). A rotor-synchronized Hahn-echo sequence was used for recording the ^{1}H MAS NMR spectra to eliminate any background signal from the probe. All ^{1}H and ^{17}O chemical shifts were referenced to 1% TMS in $CDCl_3$ and neat D_2O(liq), respectively. Solid-state ^{7}O NMR spectra were collected at 16.4, 18.8, and 21.1 T. At 16.4 T, a Bruker 2.5 mm HX MAS probe was used. A rotor-synchronized Hahn-echo sequence was used for recording ^{17}O MAS NMR spectra to eliminate the acoustic ringing effect. The 90° pulse width for the ^{17}O central transition was 1.0 μs. The 2D ^{17}O triple-quantum (3Q) MAS spectra were acquired for **2** and **3** at 18.8 T and **4** at 21.1 T, using Bruker Avance III spectrometers and Low-E 3.2 mm HXY MAS probes designed and constructed at the National High Magnetic Field Laboratory (NHMFL, Tallahassee, FL, USA). A shifted-echo SPAM 3QMAS pulse sequence[88,89] was used with 3Q excitation and conversion pulses of 3.3 and 1.1 μs at an rf field of ∼125 kHz, "soft" $\pi/2$- and π-pulses of 10 and 20 μs at an rf field of 8.3 kHz, and rotor-synchronized indirect dimension f_1 spectral windows at a sample spinning frequency of 16 kHz. Spectral folding due to the limited f_1 spectral window was resolved by Q-shearing, zero-filling in the frequency domain, and then shearing into the conventional isotropic 3QMAS representation.[90] The total experiment times for the 2D 3QMAS spectra of **2**, **3**, and **4** were approximately 19, 55, and 38 h, respectively.

3. RESULTS AND DISCUSSION

Figure 1 displays the molecular structures of compounds **1**−**4**. The reason we chose to study these compounds was based on well-documented crystal structures of these or related compounds in the literature: **1** (CCDC 2052354,

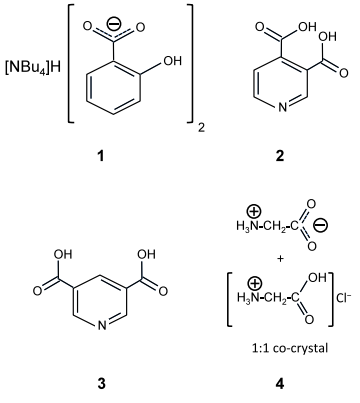

Figure 1. Molecular structures of compounds **1**−**4**.

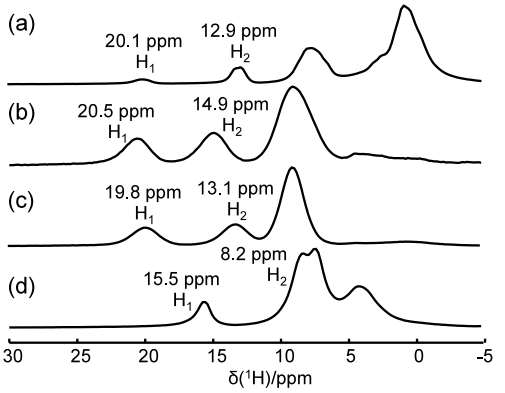

Figure 2. ^{1}H MAS NMR spectra of (a) **1**, (b) **2**, (c) **3**, and (d) **4**. All spectra were obtained at 16.4 T with a sample spinning frequency of 30 kHz. In each case, a total of 16 transients were collected with a recycling delay of 60 s.

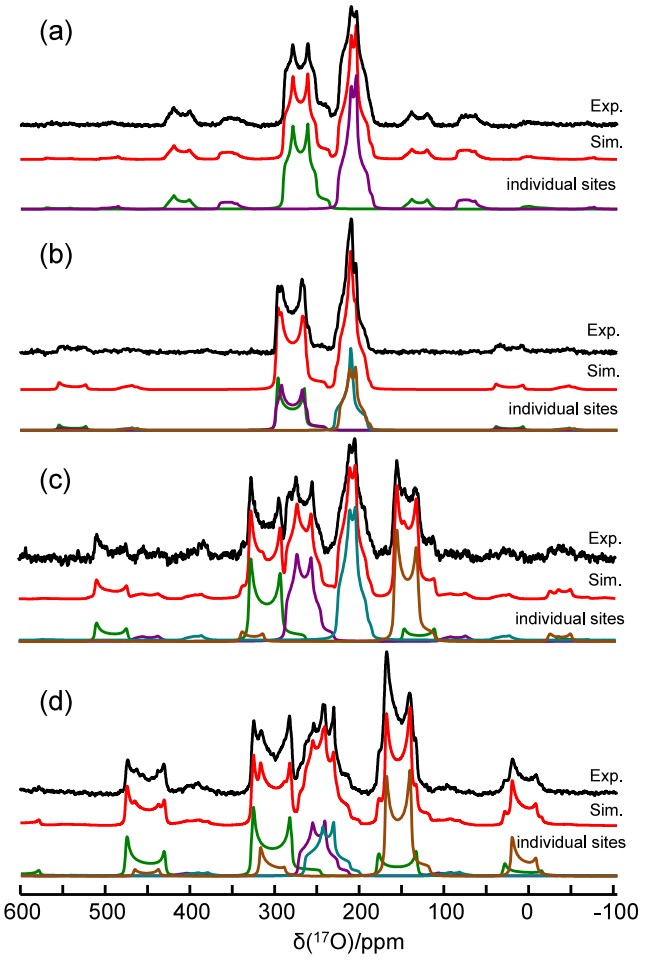

Figure 3. Experimental (black trace) and simulated (red trace) ^{17}O MAS NMR spectra of (a) **1**, (b) **2**, (c) **3**, and (d) **4**. For easy comparison, subspectra (green, purple, turquoise, and brown traces) from individual sites are also shown. The spectra shown in (a) and (d) were obtained at 18.8 T, whereas those in (b) and (c) were acquired at 21.1 T. The sample spinning frequencies were (a) 17.00, (b) 31.25, (c) 22.00, and (d) 16.00 kHz. Other acquisition parameters are (a) 4096 transients, 0.5 s recycle delay; (b) 3072 transients, 30 s recycle delay; (c) 3072 transients, 30 s recycle delay; (d) 4096 transients, 1 s recycle delay.

https://doi.org/10.1021/acs.jpca.4c01866
J. Phys. Chem. A 2024, 128, 4288−4296

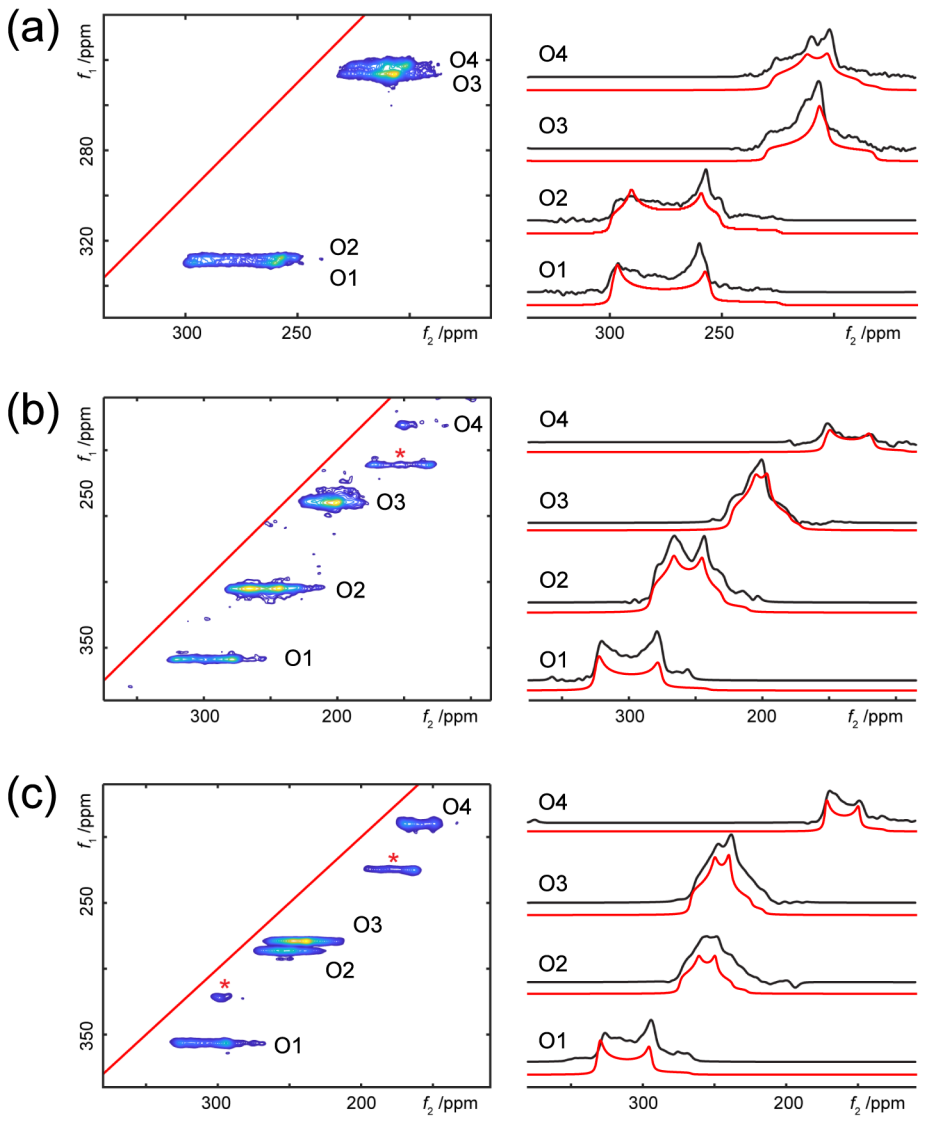

Figure 4. Left panel: experimental 2D ^{17}O 3QMAS NMR spectra of (a) **2**, (b) **3**, and (c) **4**. Right panel: corresponding experimental (black trace) and simulated (red trace) slice spectra. The 2D spectra shown in (a) and (b) were obtained at 18.8 T, whereas the 2D spectrum in (c) was acquired at 21.1 T. The sample spinning frequency was 16 kHz in all three cases. The signals marked with an asterisk are spinning sidebands. The red line shown in each 2D spectrum corresponds to the "chemical shift axis," where the f_1/f_2 slope is 1.

129904),[91,92] **2** (CCDC 1245595),[93] **3** (CCDC 1141283),[94] and **4** (CCDC 1139935).[95] In particular, each of these compounds exhibits a CBHB network in the crystal lattice. However, before we examine the structural details of these compounds, we will first present solid-state ^{1}H and ^{17}O NMR results. Figure 2 shows the ^{1}H MAS NMR spectra of compounds **1**−**4**. In each case, the ^{1}H NMR signals for protons involved in the CBHB network are indicated. Their assignments are based on an established correlation between $\delta_{iso}(^1H)$ and the HB distance (vide infra). Before we discuss these results further in the next section, it is important to note at this time that the $\delta_{iso}(^1H)$ values found for the hydrogen-bonded protons in these compounds span a wide range (from 20.5 ppm for H_1 in **2** to 8.2 ppm for H_2 in **4**), reflecting quite different HB environments in these compounds.

Figure 3 displays the ^{17}O MAS NMR spectra for compounds **1**−**4**. For compound **1**, two well-resolved ^{17}O NMR signals are observed. Using a standard spectral analysis,[49] we obtained the following set of ^{17}O NMR parameters, $\delta_{iso}(^{17}O)$, C_Q, and η_Q, for each O site in this compound. However, as seen in Figure 3, the ^{17}O MAS NMR spectra for compounds **2**−**4** are rather complex because, in each of these compounds, there are four different O sites, whose signals are partially or severely overlapped. We also obtained ^{17}O MAS spectra at 16.4 T for all four compounds (see Figure S1). To aid the final spectral analysis for compounds **2**−**4**, we obtained 2D ^{17}O 3QMAS spectra. As seen in Figure 4, each of the four O sites can be resolved and analyzed separately. Final ^{17}O NMR parameters obtained for compounds **1**−**4** are listed in Table 1. An independent check for the quality of all the ^{17}O NMR parameters listed in Table 1 is to examine the peak positions observed in the isotropic dimension of the 3QMAS spectra.[96] Indeed excellent agreement was observed between the experimental and calculated peak positions; see Figure S2.

Now it is time to examine structural details of the CBHB networks in compounds **1**−**4** and investigate how the ^{1}H and ^{17}O NMR parameters are influenced by HB interactions. Figure 5 displays partial crystal structures of compounds **1**−**4** to highlight the CBHB networks; crystal packing within the entire

https://doi.org/10.1021/acs.jpca.4c01866
J. Phys. Chem. A 2024, 128, 4288−4296

Table 1. A Summary of Experimental Solid-State ^{1}H and ^{17}O NMR Parameters Obtained for Compounds 1−4[a]

compound	$\delta_{iso}(^{1}H)$ (ppm)	$\delta_{iso}(^{17}O)$ (ppm)	C_Q (MHz)	η_Q	$\delta_{3Q,iso}$ (ppm calc.)[b]	$\delta_{3Q,iso}$(ppm expt.)
1						
H_1	20.1					
H_2	12.9					
O_1		295	7.5	0.35		
O_2		228	6.2	0.70		
2						
H_1	20.5					
H_2	14.9					
O_1		308	8.2	0.05	329.1	329.9
O_2		307	8.0	0.20	328.0	327.7
O_3		231	5.7	1.00	244.4	246.3
O_4		225	6.0	0.60	238.3	242.7
3						
H_1	19.8					
H_2	13.1					
O_1		340	8.7	0.05	363.7	358.8
O_2		290	7.6	0.40	310.2	304.9
O_3		227	6.2	0.65	241.4	240.0
O_4		166	7.3	0.15	183.2	180.8
4						
H_1	15.5					
H_2	8.2					
O_1		341	8.6	0.05	359.1	356.5
O_2		276	6.8	0.50	289.0	286.3
O_3		268	7.0	0.60	282.2	279.2
O_4		180	6.9	0.00	191.5	190.0

[a]The uncertainties in experimental $\delta_{iso}(^{1}H)$, $\delta_{iso}(^{17}O)$, C_Q, and η_Q values are ±0.1 ppm, ±1 ppm, ± 0.1MHz, and ±0.05, respectively. [b]$\delta_{3Q,iso}$ (expressed in ppm) is defined as: $\delta_{3Q,iso} = \delta_{iso} + \left(\frac{3}{850}\right)\left(1 + \frac{\eta_Q}{3}\right)\left(\frac{C_Q}{\nu_0}\right) \times 10^6$, where ν_0 is the Larmor frequency for ^{17}O.

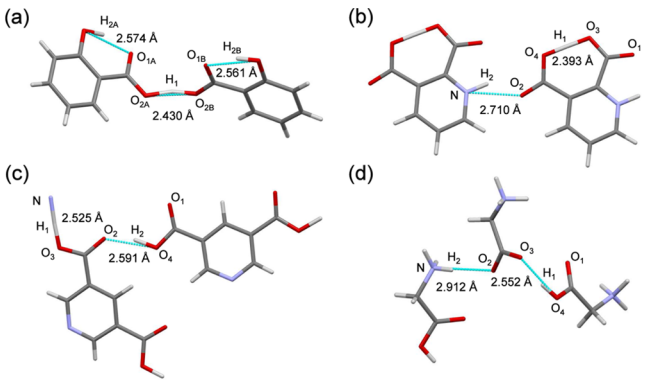

Figure 5. Partial crystal structures of (a) **1**, (b) **2**, (c) **3**, and (d) **4** to illustrate the CBHB networks in these compounds. Color coding for atoms: H (white), C (gray), N (light blue), and O (red). Relevant HB lengths are shown.

unit cell is illustrated in Figure S3. As seen in Figure 5, the two salicylate anions in **1** are linked by a central HB forming a CBHB network.[91] Here, we assumed that the crystal structure of **1** is isostructural to those of the related compounds: 1-ethyl-2,3-dimethylimidazolium hydrogen disalicylate (CCDC 2052354)[91] and 8-hydroxyquinolinium hydrogen disalicylate (CCDC 129904).[92] Interestingly, in these acid salt compounds, the central $O_{2A}\cdots H_1\cdots O_{2B}$ HB has a very short HB distance (about 2.430 Å) and is nearly symmetric. This is consistent with the observation that the H_1 proton in **1** has a $\delta_{iso}(^{1}H)$ value of 20.1 ppm. The other type of HB in **1** corresponds to a weak $O-H_2\cdots O$ HB. Thus, the CBHB network in **1** can be denoted as $O-H_{2A}\cdots O_{1A}-C-O_{2A}\cdots H_1\cdots O_{2B}-C-O_{1B}\cdots H_{2B}-O$. The crystal structure of **2** (CCDC 1245595) also displays a CBHB network but is largely within the same molecule.[93] The HB of the $O_3\cdots H_1\cdots O_4$ in **2** is among the shortest found in the literature. But the neutron diffraction crystal structure of **2** suggests that this HB is asymmetric (the $O_4\cdots H_1$ distance is 1.163 Å, whereas the $H_1\cdots O_3$ distance is 1.238 Å).[93] The H_1 displays a $\delta_{iso}(^{1}H)$ value of 20.5 ppm. In comparison, the $N-H_2\cdots O$ HB is much weaker, with a corresponding $\delta_{iso}(^{1}H)$ value of 14.9 ppm. We can denote the CBHB network in **2** as $N-H_2\cdots O_2-C-O_4\cdots H_1\cdots O_3-C-O_1$. This CBHB network is identical to what was discussed earlier in the protein structure of 1k7c; see Scheme 2. As also seen in Figure 5, the CBHB network in **3** (CCDC 1141283) is somewhat different, where the strongest HB is of the type $O\cdots H_1\cdots N$.[94] For this HB, the O···N distance is 2.525 Å, which is among the shortest O···N HBs found in the literature. The CBHB network in **3** can be identified as $N\cdots H_1\cdots O_3-C-O_2\cdots H_2-O_4-C-O_1$. This is very similar to that seen in the protein structure 4kxw shown in Scheme 2. The crystal structure of **4** (CCDC 1139935) suggests that the CBHB network in this compound is formed among three Gly molecules.[95] While the $O_4-H_1\cdots O_3$ HB is reasonably strong (with the $O_4\cdots O_3$ distance of 2.552 Å), the $N-H_2\cdots O_2$ HB is very weak. As a result, the $\delta_{iso}(^{1}H)$ values for H_1 and H_2 are 15.5 and 8.2 ppm, respectively. The CBHB network in **4** can be denoted as $N-H_2\cdots O_2-C-O_3\cdots H_1-O_4-C-O_3$. This arrangement is also similar to that seen in **3**.

After having established the ^{1}H and ^{17}O NMR signal identities and their relationships with the CBHB geometry for each of the compounds, it is highly desirable to have a simple way of visualization for all of the ^{1}H and ^{17}O chemical shift results. To

https://doi.org/10.1021/acs.jpca.4c01866
J. Phys. Chem. A 2024, 128, 4288−4296

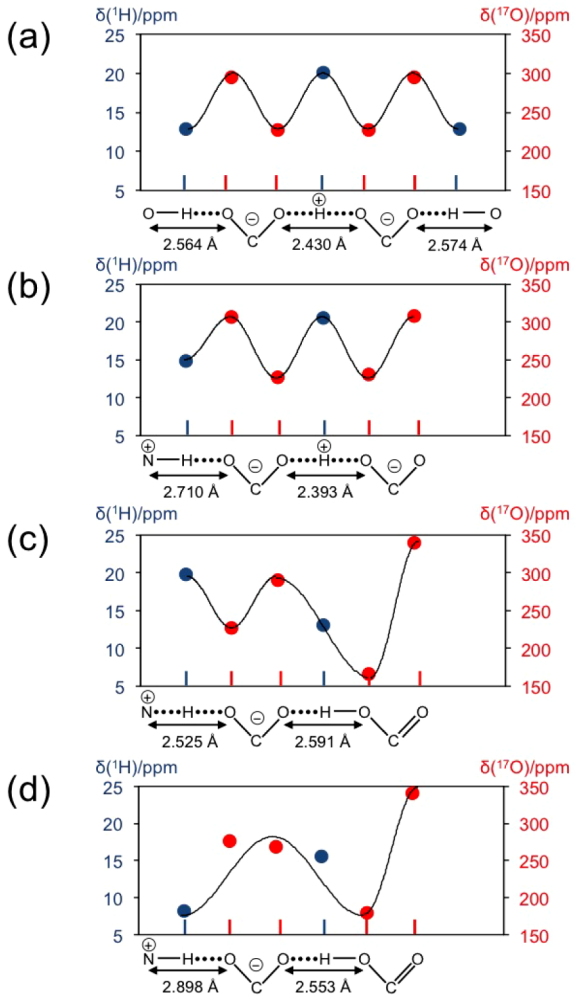

Figure 6. Illustration of the "$^{1}H/^{17}O$ chemical shift waves" observed in (a) **1**, (b) **2**, (c) **3**, and (d) **4**. The horizontal axis corresponds to the atomic positions of the H (blue) and the O (red) atoms along the CBHB network for each compound.

this end, we set out to design a simple graphical representation, in which the observed ^{1}H and ^{17}O chemical shifts are displayed according to the H and O atomic positions appearing along the CBHB network. As illustrated in Figure 6, because compound **1** has a CBHB network of the type O−H···O−C−O···H···O−C−O···H−O, there are three H atoms with two distinct $\delta_{iso}(^{1}H)$ values and four carboxylate O atoms with two distinct $\delta_{iso}(^{17}O)$ values. When the color-coded data points are connected, a "wavy" pattern appears. In this study, we refer to this kind of wavy pattern along a CBHB network as "$^{1}H/^{17}O$ chemical shift waves." This term is analogous to the known concepts of "dipolar waves" and "chemical shift waves" that are often used for describing the $^{1}H-^{15}N$ dipolar couplings and ^{1}H or ^{15}N chemical shifts along the protein backbone for oriented transmembrane peptides.[97−100] Here, we follow the ^{1}H and ^{17}O chemical shifts along the atomic chain that forms the CBHB network. However, it is important to point out that both dipolar and chemical shift waves are perfect sine waves. In the present case, there is no underlying principle suggesting that the $^{1}H/^{17}O$ chemical shift waves must be sine waves. Rather, the use of sine waves to mimic the observed wavy patterns is simply to guide the eye for easy visualization and pattern recognition. At this time, we note a few general features in the $^{1}H/^{17}O$ chemical shift waves. First, the plotting range for $\delta_{iso}(^{1}H)$ is between 5 and 25 ppm, which covers essentially the whole $\delta_{iso}(^{1}H)$ range for all H atoms involved in HBs. Second, the range for $\delta_{iso}(^{17}O)$ is between 150 and 350 ppm. Once again, all ^{17}O chemical shifts observed for carboxylic acid functional groups fall into this range. Third, if a blue data point for $\delta_{iso}(^{1}H)$ lies at the peak of a $^{1}H/^{17}O$ chemical shift wave, this feature indicates that this H atom is involved in a very strong HB. Fourth, the relative positions between two adjacent red data points are a direct measure of the ionization state of a carboxylate group. More specifically, if two adjacent red data points are close to one another (e.g., with a difference of $\delta_{iso}(^{17}O)$ values of less than 50 ppm), the two O atoms must belong to a carboxylate COO^{-} group. If the two adjacent red data points are far apart (e.g., with a difference of $\delta_{iso}(^{17}O)$ values close to 200 ppm), the two O atoms then belong to a neutral COOH group.

It is also interesting to note that the $^{1}H/^{17}O$ chemical shift waves observed for compounds **1**−**4** can be divided into two general types. One is that observed for compounds **1** and **2** as seen in Figure 6a,b, and the other is the type displayed by compounds **3** and **4** in Figure 6c,d. In the first type, the characteristic feature is that a blue data point appears as the peak of the wave flanked by two red data points, whereas in the second type, a blue data point appears on a slope between the two red data points. The structural reasons for these two types of $^{1}H/^{17}O$ chemical shift waves are quite clear. To give rise to the first type, one side of the bridging carboxyl group must be involved in a very strong H···O HB, and the other side has a rather weak one. If the HB interactions on both sides of the bridging carboxyl group are relatively weak, then the second type will be observed. On the basis of this observation, one may be able to predict that proteins of 1k7c and 4kxw should display the first type of $^{1}H/^{17}O$ chemical shift waves, and that the protein of 5mop should give rise to the second type; see Scheme 2.

4. CONCLUSIONS

We obtained extensive solid-state ^{1}H and ^{17}O NMR parameters for four organic compounds each consisting of a CBHB network. One common feature in these characteristic CBHB networks is that very often multiple strong HBs are linked together. Thus, the solid-state ^{1}H and ^{17}O NMR parameters observed for CBHB networks are very different from those seen in the most commonly found carboxylic acid dimers. We have introduced a simple graphical representation to illustrate how ^{1}H and ^{17}O chemical shift data can display a $^{1}H/^{17}O$ chemical shift wave along the CBHB network. This is the first attempt to simultaneously examine ^{1}H and ^{17}O chemical shifts from the perspective, where the H and the O atoms are linked to form an extended HB network. Because CBHB networks are commonly found in proteins, this study offers a glimpse of what might be expected in solid-state ^{1}H and ^{17}O NMR spectra for proteins. While we focused only on ^{1}H and ^{17}O chemical shifts in the present study, it is conceivable that the concept of $^{1}H/^{17}O$ chemical shift waves may be extended to include all other atoms in the entire HB network (e.g., ^{1}H, ^{17}O, ^{13}C, and ^{15}N chemical shifts for the CBHB network).

■ ASSOCIATED CONTENT

Supporting Information

The Supporting Information is available free of charge at https://pubs.acs.org/doi/10.1021/acs.jpca.4c01866.

https://doi.org/10.1021/acs.jpca.4c01866
J. Phys. Chem. A 2024, 128, 4288−4296

Experimental and simulated ^{17}O MAS NMR spectra of compounds **1**−**4** at 16.4 T; comparison between observed and calculated signal positions in the ^{17}O 3QMAS spectra for compounds **2**−**4**; diagrams showing crystal packing within the unit cell in compounds **1**−**4** (PDF)

AUTHOR INFORMATION

Corresponding Author

Gang Wu − *Department of Chemistry, Queen's University, Kingston, Ontario K7L 3N6, Canada;* orcid.org/0000-0002-0936-9432; Email: wugang@queensu.ca

Authors

Yizhe Dai − *Department of Chemistry, Queen's University, Kingston, Ontario K7L 3N6, Canada*

Ivan Hung − *National High Magnetic Field Laboratory, Tallahassee, Florida 32310, United States;* orcid.org/0000-0001-8916-739X

Zhehong Gan − *National High Magnetic Field Laboratory, Tallahassee, Florida 32310, United States;* orcid.org/0000-0002-9855-5113

Victor Terskikh − *Metrology, National Research Council Canada, Ottawa K1A 0R6, Canada;* orcid.org/0000-0003-1514-2610

Complete contact information is available at: https://pubs.acs.org/10.1021/acs.jpca.4c01866

Notes

The authors declare no competing financial interest.

ACKNOWLEDGMENTS

This work was supported by the Natural Sciences and Engineering Research Council (NSERC) of Canada through a discovery grant to GW (RGPIN: 03140-2021). A portion of this work was performed at the National High Magnetic Field Laboratory (NHMFL), which is supported by the National Science Foundation Cooperative Agreement (DMR-2128556, DMR-1644779) and the State of Florida. The NMR user facility at the NHMFL is also supported by NIH P41GM122698 and RM1GM148766. Access to the 21.1 T NMR spectrometer was provided by the Government of Canada Ultrahigh-Field NMR Collaboration Platform, operated by the National Research Council Canada with support from Laboratories Canada, and a consortium of other Canadian Government Departments and Universities. We thank Dr. Xianqi Kong for assistance in the synthesis of [$^{17}O_4$]dinicotinic acid.

REFERENCES

(1) Huggins, M. L. Hydrogen bridges in organic compounds. *J. Org. Chem.* **1936**, *1* (5), 407−456.

(2) Hendricks, S. B. The orientation of the oxalate group in oxalic acid and some of its salts. *Z. Kristallogr.* **1935**, *91*, 48−64.

(3) Derissen, J. L.; Smith, P. H. Refinement of the crystal structures of anhydrous α- and β-oxalic acids. *Acta Crystallogr., Sect. B* **1974**, *30*, 2240−2242.

(4) Leiserowitz, L. Molecular packing modes. Carboxylic acids. *Acta Crystallogr.* **1976**, *B32*, 775−802.

(5) D'Ascenzo, L.; Auffinger, P. A comprehensive classification and nomenclature of carboxyl-carboxyl(ate) supramolecular motifs and related catemers: Implications for biomolecular systems. *Acta Crystallogr., Sect. B* **2015**, *71*, 164−175.

(6) Langkilde, A.; Kristensen, S. M.; Lo Leggio, L.; Molgaard, A.; Jensen, J. H.; Houk, A. R.; Kauppinen, S.; Larsen, S. Short strong hydrogen bonds in proteins: A case study of rhamnogalacturonan acetylesterase. *Acta Crystallogr., Sect. D* **2008**, *64*, 851−863.

(7) Lin, J.; Pozharski, E.; Wilson, M. A. Short carboxylic acid−carboxylate hydrogen bonds can have fully localized protons. *Biochemistry* **2017**, *56*, 391−402.

(8) Dai, S.; Funk, L.-M.; von Pappenheim, F. R.; Sautner, V.; Paulikat, M.; Schröder, B.; Uranga, J.; Mata, R. A.; Tittmann, K. Low-barrier hydrogen bonds in enzyme cooperativity. *Nature* **2019**, *573*, 609−613.

(9) Schiebel, J.; Gaspari, R.; Wulsdorf, T.; Ngo, K.; Sohn, C.; Schrader, T. E.; Cavalli, A.; Ostermann, A.; Heine, A.; Klebe, G. Intriguing role of water in protein-ligand binding studied by neutron crystallography on trypsin complexes. *Nat. Commun.* **2018**, *9*, 3559.

(10) Smith, R.; Brereton, I. M.; Chai, R. Y.; Kent, S. B. H. Ionization states of the catalytic residues in HIV-1 protease. *Nat. Struct. Biol.* **1996**, *3*, 946−950.

(11) Piana, S.; Sebastiani, D.; Carloni, P.; Parrinello, M. Ab Initio molecular dynamics-based assignment of the protonation state of pepstatin A/HIV-1 protease cleavage site. *J. Am. Chem. Soc.* **2001**, *123*, 8730−8737.

(12) Das, A.; Mahale, S.; Prashar, V.; Bihani, S.; Ferrer, J. L.; Hosur, M. V. X-ray snapshot of HIV-1 protease in action: Observation of tetrahedral intermediate and short ionic hydrogen bond SIHB with catalytic aspartate. *J. Am. Chem. Soc.* **2010**, *132*, 6366−6373.

(13) Hayashi, S.; Umemura, J. Disappearances of COOH infrared bands of benzoic acid. *J. Chem. Phys.* **1974**, *60*, 2630−2633.

(14) Nagaoka, S.; Terao, T.; Imashiro, F.; Saika, A.; Hirota, N.; Hayashi, S. A study on the proton transfer in the benzoic acid dimer by carbon-13 high-resolution solid-state NMR and proton T1 measurements. *Chem. Phys. Lett.* **1981**, *80*, 580−584.

(15) Meier, B. H.; Graf, F.; Ernst, R. R. Structure and dynamics of intramolecular hydrogen bonds in carboxylic acid dimers: A solid state NMR study. *J. Chem. Phys.* **1982**, *76*, 767−774.

(16) Nagaoka, S.; Terao, T.; Imashiro, F.; Saika, A.; Hirota, N.; Hayashi, S. An NMR relaxation study on the proton transfer in the hydrogen bonded carboxylic acid dimers. *J. Chem. Phys.* **1983**, *79*, 4694−4703.

(17) Meier, B. H.; Meyer, R.; Ernst, R. R.; Stockli, A.; Furrer, A.; Haelg, W.; Anderson, I. The mechanism of proton dynamics in solid carboxylic acids. Reply to the comment by K. Furic. *Chem. Phys. Lett.* **1984**, *108*, 522−523.

(18) Gough, A.; Haq, M. M. I.; Smith, J. A. S. The mechanism of proton transfer in carboxylic acid dimers as studied by ^{17}O quadrupole double resonance. *Chem. Phys. Lett.* **1985**, *117*, 389−393.

(19) Meyer, R.; Ernst, R. R. Hydrogen transfer in double minimum potential: Kinetic properties derived from quantum dynamics. *J. Chem. Phys.* **1987**, *86*, 784−801.

(20) Jarvie, T. P.; Thayer, A. M.; Millar, J. M.; Pines, A. Effect of correlated proton jumps on the zero field NMR spectrum of solid p-toluic acid. *J. Phys. Chem.* **1987**, *91*, 2240−2242.

(21) Skinner, J. L.; Trommsdorff, H. P. Proton transfer in benzoic acid crystals: A chemical spin-boson problem. Theoretical analysis of nuclear magnetic resonance, neutron scattering, and optical experiments. *J. Chem. Phys.* **1988**, *89*, 897−907.

(22) Horsewill, A. J.; Aibout, A. The dynamics of hydrogen atoms in the hydrogen bonds of carboxylic acid dimers. *J. Phys.: Condens. Matter.* **1989**, *1*, 9609−9622.

(23) Oppenlander, A.; Rambaud, C.; Trommsdorff, H. P.; Vial, J.-C. Vial Translational tunneling of protons in benzoic-acid crystals. *Phys. Rev. Lett.* **1989**, *63*, 1432−1435.

(24) Meyer, R.; Ernst, R. R. Transitions induced in a double minimum system by interaction with a quantum mechanical heat bath. *J. Chem. Phys.* **1990**, *93*, 5518−5532.

(25) Stockli, A.; Meier, B. H.; Kreis, R.; Meyer, R.; Ernst, R. R. Hydrogen bond dynamics in isotopically substituted benzoic acid dimers. *J. Chem. Phys.* **1990**, *93*, 1502−1520.

(26) Cukier, R. I.; Morillo, M. A theoretical analysis of nuclear magnetic resonance experiments on proton transfer in benzoic acid crystals. *J. Chem. Phys.* **1990**, *93*, 2364−2369.

(27) Heuer, A.; Haeberlen, U. The dynamics of hydrogens in double-well potentials: the transition of the jump rate from the low-temperature quantum-mechanical to the high-temperature activated regime. *J. Chem. Phys.* **1991**, *95*, 4201−4214.
(28) Robyr, P.; Meier, B. H.; Ernst, R. R. Tensor correlation by 2D spin-diffusion powder NMR spectroscopy: Determination of the asymmetry of the hydrogen-bond potential in benzoic acid. *Chem. Phys. Lett.* **1991**, *187*, 471−478.
(29) Takeda, S.; Tsuzumitani, A.; Chatzidimitriou-Dreismann, C. A. Evidence of quantum correlations in the H/D-transfer dynamics in the hydrogen bonds in partially deuterated benzoic acid crystals. *Chem. Phys. Lett.* **1992**, *198*, 316−320.
(30) Horsewill, A. J.; Heidemann, A.; Hayashi, S. Hydrogen bond dynamics in dodecanoic acid studied by QNS and NMR. *Z. Phys. B: Condens. Matter.* **1993**, *90*, 319−324.
(31) Brougham, D. F.; Horsewill, A. J.; Ikram, A.; Ibberson, R. M.; McDonald, P. J.; Pinter-Krainer, M. The correlation between hydrogen bond tunneling dynamics and the structure of benzoic acid dimers. *J. Chem. Phys.* **1996**, *105*, 979−982.
(32) Takeda, S.; Tsuzumitani, A. An indication of slowing down of hydrogen atom transfer in isotopically mixed hydrogen bonds of benzoic acid crystals. *Magn. Reson. Chem.* **2001**, *39*, S44−S49.
(33) Fillaux, F.; Limage, M. H.; Romain, F. Quantum proton transfer and interconversion in the benzoic acid crystal: Vibrational spectra, mechanism and theory. *Chem. Phys.* **2002**, *276*, 181−210.
(34) Horsewill, A. J.; McGloin, C. J.; Trommsdorff, H. P.; Johnson, M. R. Proton tunnelling in the hydrogen bonds of halogen-substituted derivatives of benzoic acid studied by NMR relaxometry: The case of large energy asymmetry. *Chem. Phys.* **2003**, *291*, 41−52.
(35) Wilson, C. C.; Goeta, A. E. Towards designing proton-transfer systems - Direct imaging of proton disorder in a hydrogen-bonded carboxylic acid dimer by variable-temperature x-ray diffraction. *Angew. Chem., Int. Ed.* **2004**, *43*, 2095−2099.
(36) Xue, Q.; Horsewill, A. J.; Johnson, M. R.; Trommsdorff, H. P. Isotope effects associated with tunneling and double proton transfer in the hydrogen bonds of benzoic acid. *J. Chem. Phys.* **2004**, *120*, 11107−11119.
(37) Fillaux, F.; Romain, F.; Limage, M.-H.; Leygue, N. Extended tunnelling states in the benzoic acid crystal: infrared and Raman spectra of the OH and OD stretching modes. *Phys. Chem. Chem. Phys.* **2006**, *8*, 4327−4336.
(38) Asaji, T.; Ueda, K.; Oguni, M. Proton dynamics in the hydrogen bonds of 4-amino-3,5-dihalogenobenzoic acid. *Chem. Phys.* **2015**, *457*, 32−36.
(39) Fillaux, F.; Cousson, A. A neutron diffraction study of the crystal of benzoic acid from 6 to 293 K and a macroscopic-scale quantum theory of the lattice of hydrogen-bonded dimers. *Chem. Phys.* **2016**, *479*, 26−35.
(40) Brunner, E.; Sternberg, U. Solid-state NMR investigations on the nature of hydrogen bonds. *Prog. Nucl. Magn. Reson. Spectrosc.* **1998**, *32*, 21−57.
(41) Horsewill, A. J. Quantum tunnelling in the hydrogen bond. *Prog. Nucl. Magn. Reson. Spectrosc.* **2008**, *52*, 170−196.
(42) Brown, S. P. Applications of high-resolution ^{1}H solid-state NMR. *Solid State Nucl. Magn. Reson.* **2012**, *41*, 1−27.
(43) Toomey, R.; Powell, J.; Cheever, J.; Harper, J. K. Distinguishing between COOH, COO^{-}, and hydrogen disordered COOH sites in solids with ^{13}C chemical shift anisotropy and T_1 measurements. *Magn. Reson. Chem.* **2024**, *62*, 190−197.
(44) Dong, S.; Ida, R.; Wu, G. A combined experimental and theoretical O-17 NMR study of crystalline urea: An example of large hydrogen-bonding effects. *J. Phys. Chem. A* **2000**, *104*, 11194−11202.
(45) Yamada, K.; Dong, S.; Wu, G. Solid-state ^{17}O NMR investigation of the carbonyl oxygen electric-field-gradient tensor and chemical shielding tensor in amides. *J. Am. Chem. Soc.* **2000**, *122*, 11602−11609.
(46) Wu, G.; Dong, S.; Ida, R.; Reen, N. A solid-state O-17 nuclear magnetic resonance study of nucleic acid bases. *J. Am. Chem. Soc.* **2002**, *124*, 1768−1777.
(47) Lemaitre, V.; Smith, M. E.; Watts, A. A review of oxygen-17 solid-state NMR of organic materials - towards biological applications. *Solid State Nucl. Magn. Reson.* **2004**, *26*, 215−235.
(48) Kwan, I. C. M.; Mo, X.; Wu, G. Probing hydrogen bonding and ion−carbonyl interactions by solid-state ^{17}O NMR spectroscopy: G-ribbon and G-quartet. *J. Am. Chem. Soc.* **2007**, *129*, 2398−2407.
(49) Wu, G. Solid-state ^{17}O NMR studies of organic and biological molecules. *Prog. Nucl. Magn. Reson. Spectrosc.* **2008**, *52*, 118−169.
(50) Wong, A.; Poli, F. Solid-state ^{17}O NMR studies of biomolecules. *Annu. Rep. NMR Spectrosc.* **2014**, *83*, 145−220.
(51) Wu, G. Solid-State ^{17}O NMR studies of organic and biological molecules: Recent advances and future directions. *Solid State Nucl. Magn. Reson.* **2016**, *73*, 1−14.
(52) Wu, G. ^{17}O NMR studies of organic and biological molecules in aqueous solution and in the solid state. *Prog. Nucl. Magn. Reson. Spectrosc.* **2019**, *114−115*, 135−191.
(53) Dai, Y.; Wu, G. Solid-state ^{17}O NMR studies of sulfonate jump dynamics in crystalline sulfonic acids: Insights into the hydrogen bonding effect. *J. Phys. Chem. A* **2020**, *124*, 9597−9604.
(54) Palmer, J.; Wu, G. Recent developments in ^{17}O NMR studies of organic and biological molecules in the solid state. *Annu. Rep. NMR Spectrosc.* **2021**, *103*, 1−46.
(55) Dong, S.; Yamada, K.; Wu, G. Oxygen-17 nuclear magnetic resonance of organic solids. *Z. Naturforsch., A* **2000**, *55*, 21−28.
(56) Howes, A. P.; Jenkins, R.; Smith, M. E.; Crout, D. H. G.; Dupree, R Influence of low-barrier hydrogen bonds on solid state ^{17}O NMR spectra of labelled phthalate species. *Chem. Commun.* **2001**, 1448−1449.
(57) Wu, G.; Yamada, K. Determination of the O-17 NMR tensors in potassium hydrogen dibenzoate: A salt containing a short O···H···O hydrogen bond. *Solid State Nucl. Magn. Reson.* **2003**, *24*, 196−208.
(58) Zhang, Q. W.; Chekmenev, E. Y.; Wittebort, R. J. ^{17}O quadrupole coupling and chemical shielding tensors in an H-bonded carboxyl group: Alpha-oxalic acid. *J. Am. Chem. Soc.* **2003**, *125*, 9140−9146.
(59) Wong, A.; Howes, A. P.; Pike, K. J.; Lemaitre, V.; Watts, A.; Anupold, T.; Past, J.; Samoson, A.; Dupree, R.; Smith, M. E. New limits for solid-state ^{17}O NMR spectroscopy: Complete resolution of multiple oxygen sites in a simple biomolecule. *J. Am. Chem. Soc.* **2006**, *128*, 7744−7745.
(60) Wong, A.; Pike, K. J.; Jenkins, R.; Clarkson, G. J.; Anupold, T.; Howes, A. P.; Crout, D. H. G.; Samoson, A.; Dupree, R.; Smith, M. E. Experimental and theoretical ^{17}O NMR study of the influence of hydrogen-bonding on C=O and O-H oxygens in carboxylic solids. *J. Phys. Chem. A* **2006**, *110*, 1824−1835.
(61) Hagaman, E. W.; Chen, B.; Jiao, J.; Parsons, W. Solid-state ^{17}O NMR study of benzoic acid adsorption on metal oxide surfaces. *Solid State Nucl. Magn. Reson.* **2012**, *41*, 60−67.
(62) Kong, X.; Shan, M.; Terskikh, V.; Hung, I.; Gan, Z.; Wu, G. Solid-state ^{17}O NMR of pharmaceutical compounds: Salicylic acid and Aspirin. *J. Phys. Chem. B* **2013**, *117*, 9643−9654.
(63) Gan, Z.; Hung, I.; Wang, X.; Paulino, J.; Wu, G.; Litvak, I. M.; Gor'kov, P. L.; Brey, W. W.; Lendi, P.; Schiano, J. L.; et al. NMR spectroscopy up to 35.2 T using a series-connected hybrid magnet. *J. Magn. Reson.* **2017**, *284*, 125−136.
(64) Metro, T.-X.; Gervais, C.; Martinez, A.; Bonhomme, C.; Laurencin, D. Unleashing the potential of ^{17}O NMR spectroscopy using mechanochemistry. *Angew. Chem., Int. Ed.* **2017**, *56*, 6803−6807.
(65) Lu, J.; Hung, I.; Brinkmann, A.; Gan, Z.; Kong, X.; Wu, G. Solid-state ^{17}O NMR reveals hydrogen-bonding energetics: Not all low-barrier hydrogen bonds are strong. *Angew. Chem., Int. Ed.* **2017**, *56*, 6166−6170.
(66) Wu, G.; Hung, I.; Gan, Z.; Terskikh, V.; Kong, X. Solid-state ^{17}O NMR study of carboxylic acid dimers: Simultaneously accessing spectral properties of low- and high-energy tautomers. *J. Phys. Chem. A* **2019**, *123*, 8243−8253.
(67) Carnahan, S. L.; Lampkin, B. J.; Naik, P.; Hanrahan, M. P.; Slowing, I. I.; Vanveller, B.; Wu, G.; Rossini, A. J. Probing O-H bonding through proton detected ^{1}H-^{17}O double resonance solid-state NMR spectroscopy. *J. Am. Chem. Soc.* **2019**, *141*, 441−450.

https://doi.org/10.1021/acs.jpca.4c01866
J. Phys. Chem. A 2024, 128, 4288−4296

(68) Chen, C.-H.; Goldberga, I.; Gaveau, P.; Mittelette, S.; Špačková, J.; Mullen, C.; Petit, I.; Métro, T.-X.; Alonso, B.; Gervais, C.; et al. Looking into the dynamics of molecular crystals of ibuprofen and terephthalic acid using ^{17}O and ^{2}H nuclear magnetic resonance analyses. *Magn. Reson. Chem.* **2021**, *59*, 975−990.
(69) Poplett, I. J. F.; Smith, J. A. S. Oxygen-17 and deuterium quadrupole double resonance in some carboxylic acid dimers. *J. Chem. Soc., Faraday Trans. 2* **1981**, *77*, 1473−1485.
(70) Seliger, J.; Zagar, V. ^{17}O nuclear quadrupole resonance study of proton disorder in solid benzoic acid, 4-hydroxybenzoic acid and 4-nitrobenzoic acid. *Chem. Phys.* **1998**, *234*, 223−230.
(71) Torkar, M.; Zagar, V.; Seliger, J. ^{1}H-^{17}O nuclear-quadrupole double-resonance study of hydrogen disorder in 2-nitrobenzoic acid. *J. Magn. Reson.* **2000**, *144*, 13−19.
(72) Hibbert, F.; Emsley, J. Hydrogen bonding and chemical reactivity. *Adv. Phys. Org. Chem.* **1990**, *26*, 255−279.
(73) Jeffrey, G. A. *An Introduction to Hydrogen Bonding*; Oxford University Press, Inc.: New York, 1997.
(74) Perrin, C. L. Are short, low-barrier hydrogen bonds unusually strong? *Acc. Chem. Res.* **2010**, *43*, 1550−1557.
(75) Schah-Mohammedi, P.; Shenderovich, I. G.; Detering, C.; Limbach, H.-H.; Tolstoy, P. M.; Smirnov, S. N.; Denisov, G. S.; Golubev, N. S. Hydrogen/Deuterium-isotope effects on NMR chemical shifts and symmetry of homoconjugated hydrogen-bonded ions in polar solution. *J. Am. Chem. Soc.* **2000**, *122*, 12878−12879.
(76) Guo, J.; Tolstoy, P. M.; Koeppe, B.; Golubev, N. S.; Denisov, G. S.; Smirnov, S. N.; Limbach, H.-H. Hydrogen bond geometries and proton tautomerism of homoconjugated anions of carboxylic acids studied via H/D isotope effects on ^{13}C NMR chemical shifts. *J. Phys. Chem. A* **2012**, *116*, 11180−11188.
(77) Fillaux, F.; Leygue, N.; Tomkinson, J.; Cousson, A.; Paulus, W. Structure and dynamics of the symmetric hydrogen bond in potassium hydrogen maleate: A neutron scattering study. *Chem. Phys.* **1999**, *244*, 387−403.
(78) Wilson, C. C.; Thomas, L. H.; Morrison, C. A. A symmetric hydrogen bond revisited: Potassium hydrogen maleate by variable temperature, variable pressure neutron diffraction and plane-wave DFT methods. *Chem. Phys. Lett.* **2003**, *381*, 102−108.
(79) Kong, X.; Brinkmann, A.; Terskikh, V.; Wasylishen, R. E.; Bernard, G. M.; Duan, Z.; Wu, Q.; Wu, G. Proton probability distribution in the O···H···O low-barrier hydrogen bond: A combined solid-state NMR and quantum chemical computational study of dibenzoylmethane and Curcumin. *J. Phys. Chem. B* **2016**, *120*, 11692−11704.
(80) Dai, Y.; Terskikh, V.; Brinmkmann, A.; Wu, G. Solid-state ^{1}H, ^{13}C, and ^{17}O NMR characterization of the two uncommon polymorphs of curcumin. *Cryst. Growth Des.* **2020**, *20*, 7484−7491.
(81) Zhu, J.; Ye, E.; Terskikh, V.; Wu, G. Solid-state ^{17}O NMR spectroscopy of large protein-ligand complexes. *Angew. Chem., Int. Ed.* **2010**, *49*, 8399−8402.
(82) Zhu, J.; Wu, G. Quadrupole central transition ^{17}O NMR spectroscopy of biological macromolecules in aqueous solution. *J. Am. Chem. Soc.* **2011**, *133*, 920−932.
(83) Tang, A. W.; Kong, X.; Terskikh, V.; Wu, G. Solid-state ^{17}O NMR of unstable acyl-enzyme intermediates: A direct probe of hydrogen onding interactions in the oxyanion hole of serine proteases. *J. Phys. Chem. B* **2016**, *120*, 11142−11150.
(84) Young, R. P.; Caulkins, B. G.; Borchardt, D.; Bulloch, D. N.; Larive, C. K.; Dunn, M. F.; Mueller, L. J. Solution-state ^{17}O quadrupole central-transition NMR spectroscopy in the active site of tryptophan synthase. *Angew. Chem., Int. Ed.* **2016**, *55*, 1350−1354.
(85) Paulino, J.; Yi, M.; Hung, I.; Gan, Z.; Wang, X.; Chekmenev, E. Y.; Zhou, H.-X.; Cross, T. A. Functional statbility of water wire-carbonyl interactions in an ion channel. *Proc. Natl. Acad. Sci. U. S. A.* **2020**, *117*, 11908−11915.
(86) Lin, B.; Hung, I.; Gan, Z.; Chien, P.-H.; Spencer, H. L.; Smith, S. P.; Wu, G. ^{17}O NMR studies of yeast ubiquitin in aqueous solution and in the solid state. *ChemBioChem* **2021**, *22*, 826−829.
(87) Holmes, J. B.; Liu, V.; Caulkins, B. G.; Hilario, E.; Ghosh, R. K.; Drago, V. N.; Young, R. P.; Romero, J. A.; Gill, A. D.; Bogie, P. M.; et al. Imaging active site chemistry and protonation states: NMR crystallography of the tryptophan synthase α-aminoacrylate intermediate. *Proc. Natl. Acad. Sci. U. S. A.* **2022**, *119*, No. e2109235119.
(88) Gan, Z.; Kwak, H.-T. Enhancing MQMAS sensitivity using signals from multiple coherence transfer pathways. *J. Magn. Reson.* **2004**, *168*, 346−351.
(89) Amoureux, J. P.; Delevoye, L.; Steuernagel, S.; Gan, Z.; Ganapathy, S.; Montagne, L. Increasing the sensitivity of 2D high-resolution NMR methods applied to quadrupolar nuclei. *J. Magn. Reson.* **2005**, *172*, 268−278.
(90) Hung, I.; Trébosc, J.; Hoatson, G. L.; Vold, R. L.; Amoureux, J.-P.; Gan, Z. Q-shear transformation for MQMAS and STMAS NMR spectra. *J. Magn. Reson.* **2009**, *201*, 81−86.
(91) Kelley, S. P.; Narita, A.; Holbrey, J. D.; Green, K. D.; Reichert, W. M.; Rogers, R. D. Understanding the effects of ionicity in salts, solvates, co-crystals, ionic co-crystals, and ionic liquids, rather than nomenclature, is critical to understanding their behavior. *Cryst. Growth Des.* **2013**, *13*, 965−975.
(92) Jebamony, J. R.; Thomas Muthiah, P. 8-Hydroxyquinolinium-salicylate-salicylic acid (1/1/1) Complex, $C_9H_8NO^+.C_7H_5O_3^-.C_7H_6O_3$. *Acta Crystallogr., Sect. C* **1998**, *54*, 539−540.
(93) Kvick, A.; Koetzle, T. F.; Thomas, R.; Takusagawa, F. Hydrogen bond studies. 85. A very short, asymmetrical, intramolecular hydrogen bond: A neutron diffraction study of pyridine-2,3-dicarboxylic acid ($C_7H_5NO_4$). *J. Chem. Phys.* **1974**, *60*, 3866−3874.
(94) Cowan, J. A.; Howard, J. A. K.; McIntyre, G. J.; Lo, S. M.-F.; Williams, I. D. Variable-temperture neutron diffraction studies of the short, strong hydrogen bonds in the crystal structure of pyridine-3,5-dicarboxylic acid. *Acta Crystallogr.* **2005**, *B61*, 724−730.
(95) Natarajan, S.; Muthukrishnan, C.; Asath Bahadur, S.; Rajaram, R. K.; Rajan, S. S. Reinvestigation of the crystal structure of diglycine hydrochloride. *Z. Kristallogr.* **1992**, *198*, 265−270.
(96) Wu, G.; Dong, S. Two-dimensional ^{17}O multiple quantum magic-angle spinning NMR of organic solids. *J. Am. Chem. Soc.* **2001**, *123*, 9119−9125.
(97) Mesleh, M. F.; Veglia, G.; DeSilva, T. M.; Marassi, F. M.; Opella, S. J. Dipolar waves as NMR maps of protein structure. *J. Am. Chem. Soc.* **2002**, *124*, 4206−4207.
(98) Kovacs, F. A.; Denny, J. K.; Song, Z.; Quine, J. R.; Cross, T. A. Helix tilt of the M2 transmembrane peptide from influenza A virus: An intrinsic property. *J. Mol. Biol.* **2000**, *295*, 117−125.
(99) Hu, J.; Asbury, T.; Achuthan, S.; Li, C.; Bertram, R.; Quine, J. R.; Fu, R.; Cross, T. A. Backbone structure of the amantadine-blocked trans-membrane domain M2 proton channel from Influenza A virus. *Biophys. J.* **2007**, *92*, 4335−4343.
(100) Wang, G. Structure, dynamics and mapping of membrane-binding residues of micelle-bound antimicrobial peptides by natural abundance ^{13}C NMR spectroscopy. *Biochim. Biophys. Acta, Biomembr.* **2010**, *1798*, 114−121.

https://doi.org/10.1021/acs.jpca.4c01866
J. Phys. Chem. A 2024, 128, 4288−4296